THE ASTROPHYSICAL JOURNAL, 351:443–453, 1990 March 10

A STUDY OF AFGL 5376: AN UNUSUAL EXTENDED INFRARED SOURCE NEAR THE GALACTIC CENTER

KEVEN UCHIDA,[1] MARK MORRIS,[1] AND E. SERABYN[2]

Received 1989 May 25; accepted 1989 September 11

ABSTRACT

We present observations of ^{12}CO $J = 2$–1 emission from AFGL 5376, an unusually warm and extended *IRAS* source located near the Galactic center, as well as from adjacent portions of the Galactic center lobe (GCL)—a radio continuum structure projecting perpendicular to the Galactic plane out to $b = 1°$. Emission at a radial velocity of 125 km s^{-1} is observed to coincide with AFGL 5376 and is apparently localized to a region of 6′ radius centered on the infrared peak. This velocity is forbidden in the sense of Galactic rotation and corresponds to that expected in this direction from the expanding molecular ring (EMR), which surrounds the Galactic nucleus at an approximate radius of 160 pc. AFGL 5376 displays a FWHM line width of 23–33 km s^{-1}, characteristic of the Galactic center cloud population. We conclude that AFGL 5376 is a molecular cloud physically located near the Galactic center, and it is probably associated with the EMR.

The *IRAS* flux ratios (60 μm/25 μm and 25 μm/12 μm) toward AFGL 5376 indicate a rather high dust color temperature of about $T_c = 100$ K ($T_d = 86$ K, assuming a dust emission efficiency factor proportional to λ^{-1}). In addition, the ^{12}CO position-velocity diagrams presented here show several abrupt velocity jumps that are possible evidence for shock discontinuities. These facts, plus the observation that AFGL 5376 is roughly coincident with the western limb of the Galactic center lobe, lead us to suggest that AFGL 5376 is being shock heated as a result of its interaction with the western lobe feature. An implication of this hypothesis is that the EMR and the western component of the GCL are physically associated in the vicinity of AFGL 5376, and we speculate that they are two manifestations of a single explosive event at the nucleus.

Subject headings: galaxies: internal motions — galaxies: nuclei — galaxies: The Galaxy — interstellar: molecules — infrared: sources

I. INTRODUCTION

Emission-line surveys carried out over the last few decades have produced kinematical evidence for highly energetic activity, both past and present, near the Galactic center (Robinson and McGee 1970; Bania 1977; Heiligman 1987; Bally *et al.* 1987). A notable example is the expanding molecular ring (EMR), an agglomeration of dense molecular clouds forming a ring tilted by 15° with respect to the Galactic plane and surrounding a 3° region containing the Galactic nucleus (Scoville 1972; Kaifu, Kato, and Iguchi 1972; Bania 1977; Cohen and Davies 1979; Güsten and Downes 1980; Sanders 1989; Güsten 1989). As its name implies, the EMR is expanding radially from the Galactic center at high velocities. Molecular features seen directly toward the Galactic nucleus at velocities of −135 km s^{-1} (Robinson and McGee 1970) and 165 km s^{-1} (Sanders and Wrixon 1974) provide evidence of this expansion and distinguish EMR clouds from others that appear to participate more or less in the overall Galactic rotation. These attributes have prompted some to suggest that the EMR is the manifestation of a highly energetic, explosive event that occurred at the Galactic center as recently as 10^6 yr ago (Scoville 1972; Kaifu, Kato, and Iguchi 1972). However, other explanations of the EMR have also been considered, such as gas in resonant orbits (Bania 1977) or the kinematical response of the gas to a rotating bar structure (Cohen and Davies 1979; Güsten and Downes 1980; Sanders 1989). Bania (1980) considers the possibility that the EMR is not a ring structure at all, but rather much of the emission associated with it is due to an expanding arm located 4 kpc behind the Galactic center

Another large-scale structure with an apparent energetic origin is the Galactic center lobe (GCL). Interest in the GCL was stirred by a map at 10.5 GHz and by a physical interpretation put forth by Sofue and Handa (1984) and Sofue (1985). The GCL has an apparent shell structure that is defined primarily by two spurs or lobes straddling the Galactic center at $l = 0.°2$ and at $l = -0.°6$ and extending nearly 1° above the Galactic plane (Fig. 1*a*). Intensity profiles across the lobes of the GCL are consistent with that of a limb-brightened shell structure (Sofue 1985). This has led to the theory that the entire GCL was produced by a channeling of gas from the Galactic plane, resulting either from energetic activity in the Galactic center (Sofue 1984, 1985; Umemura *et al.* 1988) or from the twisting of poloidal magnetic field lines by Galactic rotation (Uchida, Shibata, and Sofue 1985). These models are summarized by Shibata (1989). It has also been suggested by Heyvaerts, Norman, and Pudritz (1988) that the GCL is the observable manifestation of a discontinuity between distributed molecular gas and a hot interior produced by coronal-like mechanisms in the Galactic center.

The western lobe of the GCL and much of the emission between the two lobes appear to be thermal in nature, in terms of their spectral index and absence of polarization (Sofue 1985; Tsuboi *et al.* 1986). However, Reich, Sofue, and Fürst (1987) argue that the western lobe is nonthermal, noting that the ratio of radio to far-IR emission is too large for a typical H II region. The eastern lobe, on the other hand, is clearly observed to contain nonthermal emission that extends continuously from the linear filaments of the Galactic center radio arc (Seiradakis *et al.* 1985; Yusef-Zadeh and Morris 1988). The polarization

[1] Department of Astronomy, University of California at Los Angeles.
[2] Division of Physics, Mathematics, and Astronomy, California Institute of Technology.

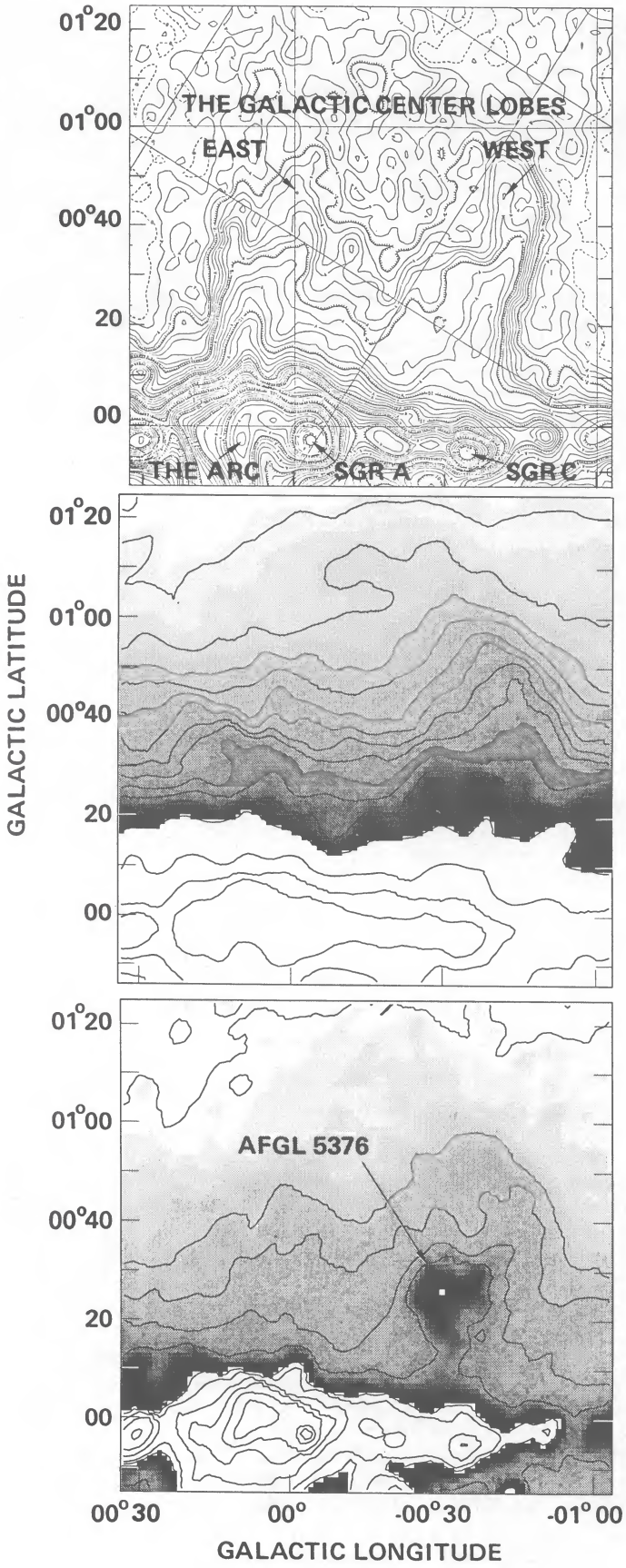

within the eastern component of the GCL is observed to be as high as 40% (Tsuboi *et al.* 1985, 1986). Existing CO observations of this region also indicate differences between the two lobe features. Sofue (1985), citing the unpublished CO data of Suwa and Fukui, reports that the western lobe is seen as a spurlike structure with velocities of 90–100 km s^{-1} while very little emission is seen from the eastern lobe. These dissimilarities between the two lobes have prompted consideration of an alternative hypothesis according to which the GCL is a superposition of two spurs that are physically unrelated (Tsuboi *et al.* 1986).

The far-infrared data of *IRAS* provide independent clues to the nature of these large-scale, energetic features. The GCL is clearly visible in all four *IRAS* bands, indicating that a dust component accompanies the radio emitting gas (Fig. 1*b*). Further evidence of the dissimilar natures of the two lobes is provided by the fact that the western lobe is much more prominent than the eastern lobe in these maps.

Another prominent feature in the Galactic center *IRAS* images is AFGL 5376 ($l = -0.^{\circ}5$, $b = 0.^{\circ}43$; Cox and Laureijs 1989; Uchida and Morris 1988). This object is one of the most striking sources in the 25 μm image (Fig. 1*c*); it is extended, approximately 6′ in radius, and nearly circularly symmetric. It does not, however, stand out noticeably above the background in the other three bands (12, 60, and 100 μm) (Fig. 1*b*), although when the background is removed, as was done in Reich, Sofue, and Fürst (1987), AFGL 5376 is apparent in the 60 μm image. AFGL 5376 is thus unusually warm; its color temperature, as determined from the *IRAS* flux ratios, is approximately 100 K (Uchida and Morris 1989).

Little else is known about AFGL 5376. This interesting structure does not appear in past radio continuum images and has been overlooked by Galactic center molecular line surveys, which have generally concentrated on regions closer to the Galactic plane ($|b| \leq 0.^{\circ}4$). AFGL 5376 was first identified in the 4, 11, 20, and 27 μm bands of the Air Force rocket surveys of the Galactic center (Little and Price 1985), where it was evident at 20 and 27 μm. No mass estimate was made from these data, but a peak $I(20)/I(27)$ color temperature of $T_c \leq 150$ K was determined.

To date, AFGL 5376 has appeared only at far-IR wavelengths. Little and Price suggested that a strong absorption feature, observed by Hiromoto *et al.* (1984) in a 0.°4 resolution, 2.4 μm survey, may correspond to AFGL 5376. However, in light of the fact that the *IRAS* observations pinpoint the peak position of AFGL 5376 at $l = -0.^{\circ}5$, $b = 0.^{\circ}43$, correspondence of the 2.4 μm absorption feature (centered at $l = -0.^{\circ}8$, $b = 0.^{\circ}6$) with AFGL 5376 appears unlikely.

A particularly interesting aspect of AFGL 5376 is that, in *IRAS* maps, it is spatially coincident with the western com-

FIG. 1.—*Top*: The Galactic center lobe, Fig. 2 from Sofue (1985), is shown in this 10.5 GHz radio continuum map of the central Galactic region. *Middle*: The infrared counterpart of the Galactic center lobe is shown in this 60 μm *IRAS* map of the central Galactic region. All three panels of the Figure are to scale. Gray values above 1.1×10^9 are blanked to reveal the isointensity contours near the Galactic plane. Contour levels = 2.8×10^7 Jy $sr^{-1} \times$ (0, 1, 3, 5, 7, 9, 11, 13, 15, 18, 22, 27, 33, 40, 80, 160, 320). Absolute flux = contour value + map bias, where map bias = 1.16×10^8 Jy sr^{-1}. *Bottom*: 25 μm *IRAS* map of AFGL 5376 and the GCL. Gray values above 1.8×10^8 are blanked to reveal the isointensity contours near the Galactic plane. Contour levels = 2.2×10^7 Jy $sr^{-1} \times$ (0, 1, 1.5, 2.5, 4, 6, 8.5, 11.5, 23, 46, 92, 184, 268). Absolute flux = contour value + map bias, where map bias = 7.66×10^7 Jy sr^{-1}.

ponent of the Galactic center lobe (Fig. 1*c*). A direct physical association between these two remarkable features would help constrain theories about the origin and nature of the GCL. Our motivation for studying AFGL 5376 is thus to determine if AFGL 5376 is physically located near the Galactic center, and if so, to use it to shed light on the nature of the GCL.

With the data presented in this paper, we examine the distribution and velocity of ^{12}CO $J = 2$–1 emission from AFGL 5376 and a few nearby regions of the GCL. We infer that AFGL 5376 is located near the Galactic center and is likely to be a part of the expanding molecular ring. Furthermore, the CO data provide evidence in support of the hypothesis based on *IRAS* data that AFGL 5376 is interacting with the Galactic center lobe. This key source thus appears to link the EMR and the GCL and is suggestive of a common origin for the two. Finally, we discuss the implications of these associations for the recent history of the most energetic Galactic center activity.

II. OBSERVATIONS

a) Equipment and Technique

The ^{12}CO $J = 2$–1 transition was observed in 1988 August with the 10.4 m antenna of the Caltech Submillimeter Observatory (CSO), located near the summit of Mauna Kea, Hawaii. The HPBW of the telescope at the transition frequency of 230 GHz was 32″. A pointing uncertainty of approximately ±3″ was achieved by periodically centering the antenna on the peak signal from Saturn. The receiver front-end was a waveguide-mounted SIS receiver (Ellison and Miller 1987). An acousto-optical spectrometer having 1024 channels and a frequency range of 500 MHz comprised the back-end. The total velocity coverage, centered on 0 km s^{-1} LSR, was ±325 km s^{-1}, and the velocity resolution was about 1.3 km s^{-1}. The average double-sideband system temperature during the observations was approximately 340 K.

The total on-source integration time for each position was 40 s, with equal time spent off the source to subtract sky emission. To avoid CO emission from the Galactic plane in the off beam, while still keeping similar elevations for the on and off beams, the off observation was positioned −75′ in R.A. from the source before transit, and +75′ in azimuth away from the source after transit.

The raw data were calibrated to produce T_A^*, the antenna temperature corrected for atmospheric absorption, with the following relation:

$$T_A^* = [(\text{on-off})/(\text{hot-off})] \times (2) \times (280)\,,$$

where "hot" is the measurement of an ambient temperature absorber (Ecosorb). Both the sky and the absorber are assumed to have a temperature of 280 K. The factor of 2 in the above relation accounts for double-sideband operation.

Baseline fluctuations were removed by fitting polynomials of order 4 or less to regions of the spectra deemed to be free of line emission. The regions of the spectra corresponding to velocity ranges of −200 to −150 km s^{-1}, 50 to 65 km s^{-1}, and 200 to 325 km s^{-1} often fulfilled this condition. Fine adjustments to these baseline windows were made on a spectrum-to-spectrum basis.

The FWHM linewidths were determined for the prominent lines. This task proved difficult, owing to the fact that many of the spectral components appeared to be self-absorbed and thus were not clearly defined. Compounding this problem was evidence for multiple spectral components that appear and disappear on small spatial scales and sometimes coexist with nearly similar velocities. These characteristics are exhibited throughout the surveyed region and may indicate the presence of clumpy turbulent material or shocks resulting from the interaction between AFGL 5376 and the surrounding medium. Thus, it was not clear whether the irregular profiles of many of the lines were caused by self-absorption, by the overlapping of multiple spectral components, or by a combination of both.

The FWHM line widths were therefore estimated by two means. Gaussian fits were used to directly determine them for a few spectral components that seemed singular and not suffering from self-absorption or blending. The values determined by this method (method 1) may be appropriate for clumps within the region studied, but for the region as a whole, they are considered lower limits. A second method (method 2) was used to estimate the FWHM of the irregular profiles that were non-Gaussian or multiply peaked. Since it was difficult to determine whether these were self-absorbed or blended profiles, we treated all such cases as if they were single self-absorbed lines. The values thus determined are regarded as upper limits to the FWHM or as a general measure of the full velocity dispersion in the region studied. These FWHM values, however, were not determined directly, because under this assumption, many of the lines appeared to have been eroded below the 50% level. Instead, possible line erosion was ignored, and the full width was measured at 20% of its peak value. Because of the steep slope of a Gaussian profile at the 20% level, the full width there is a close approximation to that of an uneroded Gaussian line profile. The FWHM values presented in this paper are derived from an assumed Gaussian profile which gives FWHM = 0.66 × (full width at 20% maximum). If the peak is reduced by a factor of 2 by self-absorption, this procedure overestimates the FWHM by only 20%, so we regard this as an estimate of the uncertainty in the upper limit values.

b) The Directions Observed

Figure 2 is a 25 μm *IRAS* map illustrating the regions surveyed. The western component of the Galactic center lobe nearly fills the entire field, and AFGL 5376 is clearly visible at ($l = -0.^\circ5$, $b = 0.^\circ43$). Table 1 summarizes the observed locations.

Since observing time was limited, compiling a grid of observations encompassing the entire region subtended by AFGL 5376 was not feasible. Instead, the observations were gathered in strips across AFGL 5376 and a few other selected areas. In most cases, the beam spacings in these strips were 1′, approximately twice the diameter of the FWHM telescope beam. Sampling on two-dimensional grids of limited size was then made over regions deemed interesting on the basis of information attained in the strip surveys.

Strips 1 and 2 consist of observations taken across the central position of AFGL 5376 at constant Galactic latitude and constant Galactic longitude, respectively. Strip 3, taken along constant latitude, cuts across the western lobe of the GCL, as defined in the 25 μm *IRAS* maps; it is located approximately 15′ north of AFGL 5376. Grid 1 (not shown in the figure) is a 2′ × 2′ grid of observations centered on the peak of AFGL 5376. Strips 4A–4D were taken along constant longitude and are centered west of the AFGL 5376 at offsets of −6.′5, −7.′5, −8.′5, and −9.′5, respectively. The zero offset position for strips 1, 2, 4A–4D, and grid 1 corresponds to the central position of AFGL 5376.

Strips 5A and 5B are observations taken along constant R.A.

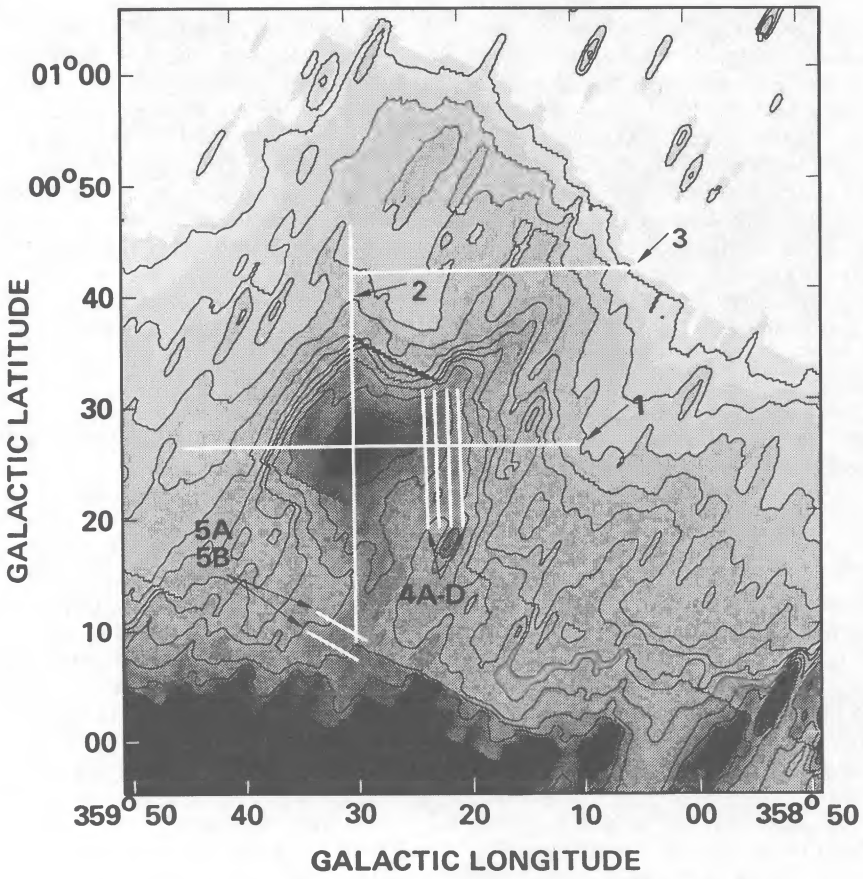

FIG. 2.—A 25 μm *IRAS* map illustrating the observations done in this study

and are centered about 15′ south of AFGL 5376 on the nonthermal radio filaments reported by Bally and Yusef-Zadeh (1989). Since the nonthermal filaments are quite narrow, these strips were fully sampled with a 0.′5 beam spacing.

III. RESULTS: POSITION-VELOCITY DIAGRAMS

Position-velocity diagrams, produced from some of the observations described above, are presented in this section. The line intensities, shown in contour format, are in units of T_A^*, the antenna temperature corrected for atmospheric absorption. The velocity resolutions of all diagrams have degraded by smoothing with a 5 km s^{-1} FWHM Gaussian.

a) Strip 1

In the longitude-velocity diagram across AFGL 5376 (Fig. 3), we see substantial emission at low velocities (−40 km

TABLE 1

OBSERVATIONS OF AFGL 5376 AND NEARBY REGIONS

Name	Zero offset Location	Number of Observations	Beam Spacing	Description
Strip 1	$l = 359.°50$ $b = 0.°43$	35	1.′0	Longitude strip across AFGL 5376
Strip 2	$l = 359.°50$ $b = 0.°43$	37	1.0	Latitude strip across AFGL 5376
Strip 3	$l = 359.°07$ $b = 0.°7$	26	1.0	Longitude strip across the GCL
GRID 1	$l = 359.°50$ $b = 0.°43$	25	1.0	5′ × 5′ grid centered on AFGL 5376
Strips 4A–4D	$l = 359.°39$, 359.°38, 359.°36, 359.°34, $b = 0.°43$	12 12 12 12	1.0	Latitude strips 6.′5, 7.′5, 8.′5, and 9.′5 west of AFGL 5376
Strips 5A, 5B	$\alpha = 17{:}40{:}36$, 17:40:45 $\delta = -29{:}13{:}00$	10 10	0.5	Declination strips across the nonthermal radio filaments

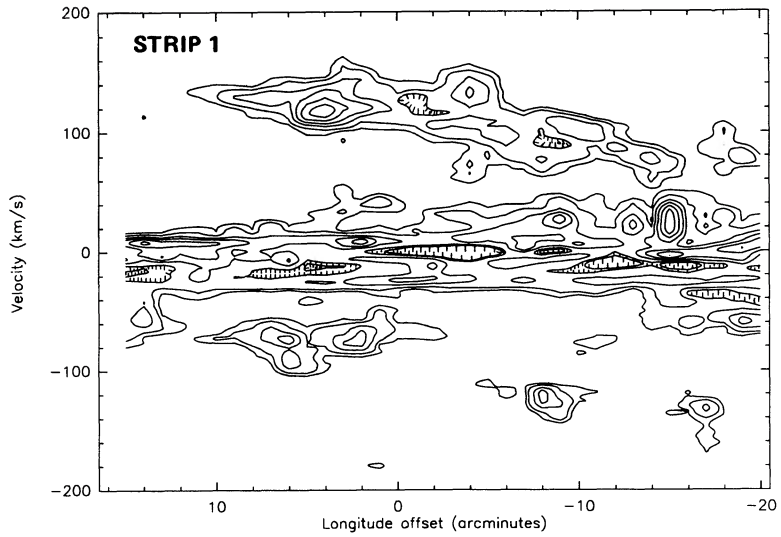

FIG. 3.—Longitude-velocity diagram across the center of AFGL 5376. Contour levels = 0.4 K × (1.0, 2.0, 4.0, 6.0, 8.5, 11.5, 15.0, 19.0, 23.5, 28.5, 34.0).

$s^{-1} < V < 40$ km s^{-1}) and over all positions. It is seen in nearly all the maps to be discussed. This band of emission at near-zero velocity is similar to that referred to by Bania (1977) as the "main maximum"; it can arise from CO located anywhere along our line of sight. Emission with velocities between -60 and -80 km s^{-1} is also seen from this and most of the other regions as well. Some of this emission might be attributed either to the nuclear disk or to the 3 kpc arm, although these features are well defined only near the Galactic plane.

Also clearly seen in strip 1 is emission with forbidden velocities ranging from 60 to 150 km s^{-1}, extending over nearly the entire longitude extent of the strip. At offsets of approximately 4′ to either side of the central position of AFGL 5376 are two pronounced intensity peaks at 120 and 130 km s^{-1} with line temperatures of 6 and 2.3 K, respectively. The 120 km s^{-1} peak is the strongest of the high positive velocity lines observed in this region. There is a distinct minimum in the antenna temperature near the center of AFGL 5376. It appears that this decrease in line strength is not due to self-absorption, because self-absorption does not explain the narrowing in the velocity extent of the emission near zero offset.

The emission near 125 km s^{-1} appears to be localized symmetrically to a region that is 6′ in radius and centered on the infrared peak of AFGL 5376. Beyond $\Delta l = 4'$, the 125 km s^{-1} component quickly diminishes in strength; it falls to less than 35% of its maximum at $\Delta l = 6'$ and completely disappears past $\Delta l = 12'$. West of AFGL's center, near $\Delta l = -6'$, a striking jump is seen in the CO velocities. This is due to the abrupt disappearance of the 125 km s^{-1} component (Fig. 4). What remains is a second distinct spectral component centered at a velocity of 100 km s^{-1}. Beyond this point ($\Delta l = -6'$), the velocity of the emission continues to decrease, eventually reaching a minimum of 75 km s^{-1} past $\Delta l = -14'$. This relatively "low" positive velocity emission appears in most of the other diagrams as well (between 60 and 120 km s^{-1}). We will sometimes refer to it as the "90 km s^{-1}" emission.

Because of the above, we associate the ($\langle V \rangle = 125$ km s^{-1}) emission with AFGL 5376. Strips 2 and 3, presented in the following sections, also provide evidence to support this assertion.

b) Strip 2

Strip 2, which crosses AFGL 5376 in latitude, also shows strong emission at forbidden velocities ranging from 70 to 180 km s^{-1} (Fig. 5). As in the longitude strip, this latitude strip shows enhancements in 125 km s^{-1} emission around the central position of AFGL 5376. These enhancements are located at $\Delta b = 2'$ and $\Delta b = -4'$, and both have a peak temperature of 4 K. The 125 km s^{-1} emission in this strip also appears to be localized to AFGL 5376. Beyond $\Delta b = 5'$, the 125 km s^{-1} emission disappears completely. Emission with velocities between 70 and 120 km s^{-1}, similar to that seen in the longitude strip, appears at offsets beyond $\Delta b = 10'$. South of AFGL 5376's center, past $\Delta b = -10'$, the emission attains velocities of up to 180 km s^{-1}.

In addition to the positive velocity features, we observe strong emission from gas at velocities between -80 and -200 km s^{-1} and at latitude offsets beyond $-12'$. The dominant spectral component from this region has an unusually large

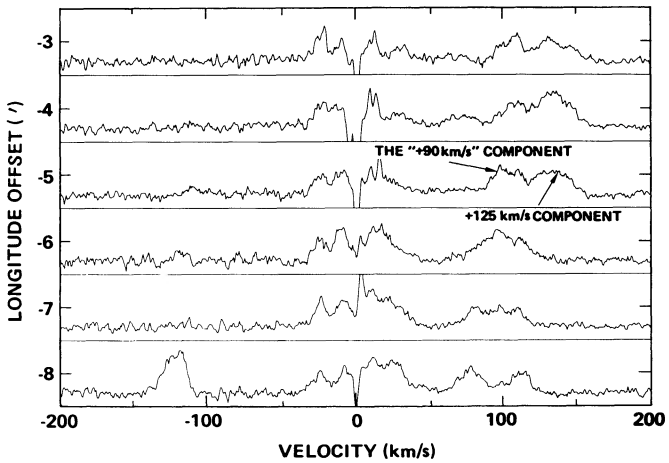

FIG. 4.—^{12}CO spectra at offsets from $\Delta l = -3'$ to $-8'$ with respect to the center of AFGL 5376. Note the sudden disappearance of the 125 km s^{-1} component at $\Delta l = -6'$.

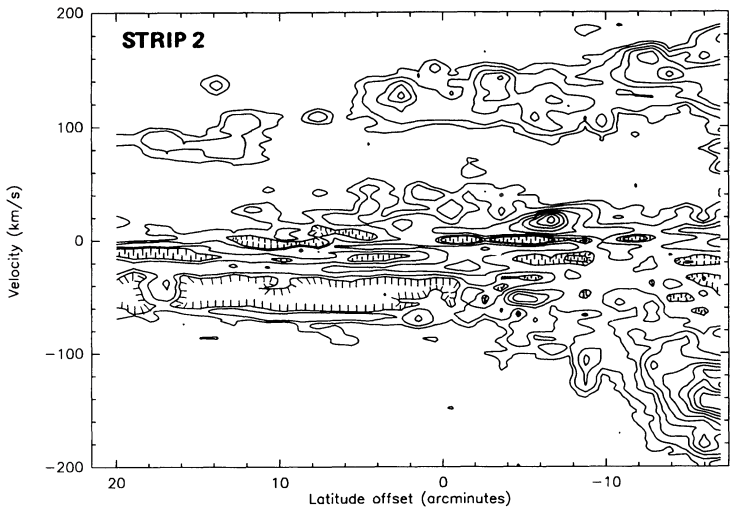

FIG. 5.—Latitude-velocity diagram across the center of AFGL 5376. Levels = 0.4 K × (1.0, 2.0, 4.0, 6.0, 8.5, 11.5, 15.0, 19.0, 23.5, 28.5, 34.0).

FWHM of about 45 km s^{-1}. This emission apparently corresponds to the -140 km s^{-1} molecular cloud reported by Bally and Yusef-Zadeh (1989).

c) Strip 3

Strip 3, the longitude-velocity strip located near the western edge of the Galactic center lobe (zero offset at $l = 359.^{\circ}07$, $b = 0.^{\circ}70$) is shown in Figure 6. With the exception of two spectra closest to AFGL 5376 at $\Delta l = 25'$ and $26'$, this strip reveals no 125 km s^{-1} emission, consistent with the localization of emission at that velocity to AFGL 5376. This region does, however, contain a clear component of emission at velocities between 50 and 100 km s^{-1} which appears intermittently between $\Delta l = 6'$ to $26'$.

d) Strip 4A

Strip 4A, a latitude strip $6'.5$ west of AFGL 5375, is presented in Figure 7. The dominant feature in this region is the "90 km s^{-1}" cloud. The 125 km s^{-1} spectral component is markedly absent from this strip, consistent with what is seen in strip 1, where 125 km s^{-1} emission is not seen beyond $\Delta l > -6'$. Strips 4B–4D, not displayed here, are similar to strip 4A.

e) The Nonthermal Radio Filaments

Strips 5A and 5B, the declination-velocity strips crossing the nonthermal filaments located approximately $15'$ south of AFGL 5376, are similar, and thus only strip 5A is illustrated (Fig. 8).

Positive velocity 110 to 160 km s^{-1} emission is seen in both strips 5A and 5B, consistent with strip 2, in which high-velocity gas (greater than 125 km s^{-1}) is seen south of AFGL 5376.

Negative velocity emission between 0 and -140 km s^{-1} is seen across the entire spatial extent of both diagrams. In addition, a spectral component centered at -140 km s^{-1} arises near $\Delta\delta = 0'.0$ and continues into negative declination offsets. The resulting velocity jump at $\Delta\delta = 0'.0$ presumably defines the edge of the -140 km s^{-1} molecular cloud hypothesized to be

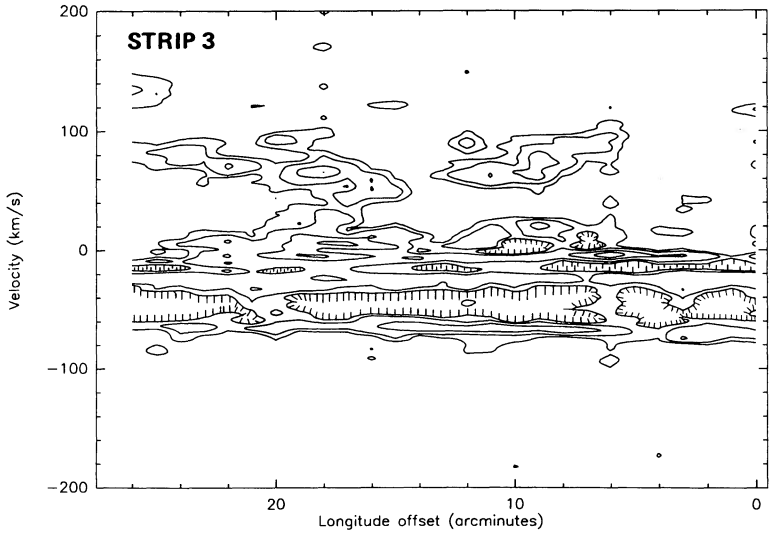

FIG. 6.—Longitude-velocity diagram across the outer edge of the western component of the GCL. The zero offset is located at ($l = 359.07$, $b = 0.7$). Levels = 0.4 K × (1.0, 2.0, 4.0, 6.0, 8.5, 11.5, 15.0, 19.0, 23.5, 28.5, 34.0).

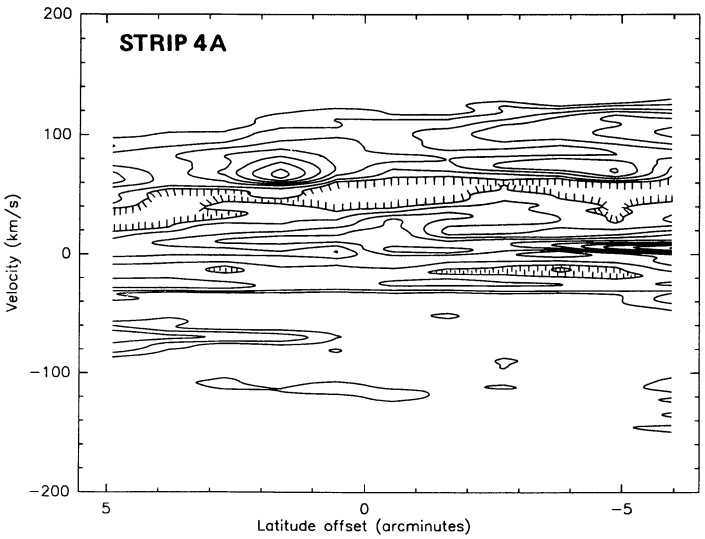

FIG. 7

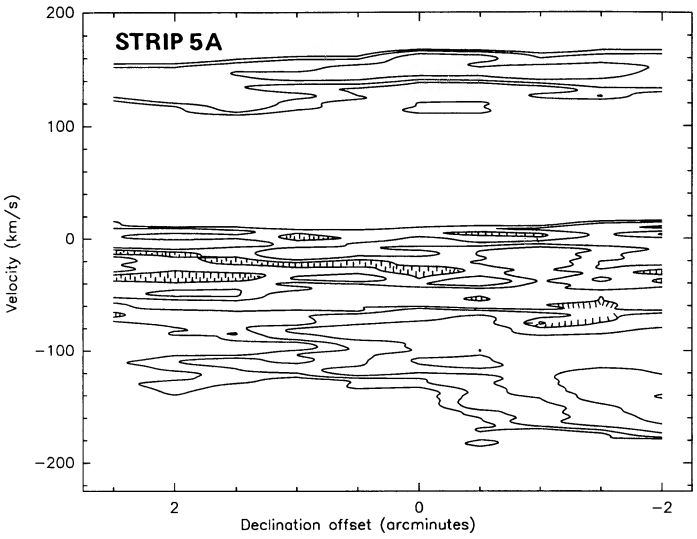

FIG. 8

FIG. 7.—Latitude-velocity diagram at an offset of $\Delta l = -6'.5$ from the central position of AFGL 5376. Levels = 0.4 K × (1.0, 2.0, 4.0, 6.0, 8.5, 11.5, 15.0, 19.0, 23.5, 28.5, 34.0).

FIG. 8.—Declination-velocity diagram across the nonthermal filaments. Levels = 0.4 K × (2.0, 3.0, 5.0, 8.0, 12.0, 17.0, 23.0, 30.0).

associated with the nonthermal radio filaments (Bally and Yusef-Zadeh 1989).

f) FWHM Line Widths

The FWHM line widths, measured as described in § II*a*, are presented in Table 2. Column (1) lists the observed regions. Column (2) provides the specific offsets over which the lines of a given radial velocity (col. [3]) were found. The lower limit (where available) and upper limit FWHM averages are presented in column (4). The 125 km s^{-1} emission from AFGL has an overall velocity breadth of 23–33 km s^{-1}.

g) Summary of Map Analysis

Figure 9 summarizes what the contour plots and position-velocity diagrams have shown thus far: that the 125 km s^{-1} emission appears to be localized to within a region of 6′ radius centered on AFGL 5376. As best determined from the two strips crossing AFGL 5376, the strongest emission appears to be concentrated in a ring that is approximately 4′ in radius and centered on the IR peak of AFGL 5376. Strip 3, which is approximately 15′ to the north of AFGL 5376, contains very little 125 km s^{-1} emission. Strips 4A–4D, which are located 6′.5–9′.5 west of AFGL 5376 (just beyond the "outer boundary" of AFGL 5376), similarly do not show a strong 125 km s^{-1} component.

Emission at velocities near 90 km s^{-1} has been noted in the majority of the regions discussed. It is located both north

TABLE 2

FWHM LINE WIDTHS

LOCATION	OFFSET RANGE	AVERAGE VELOCITY (km s^{-1})	FWHM (km s^{-1}) Method 1	FWHM (km s^{-1}) Method 2
Strip 1	$-5' \le \Delta l \le 15'$	125	18	29
	$-20' \le \Delta l \le -6'$	90	18	24
Strip 2	$-17' \le \Delta l \le -13'$	−140	45	56
	$-17' \le \Delta l \le -10'$	>125	...	38
	$-9' \le \Delta l \le 6'$	125	...	34
	$7' \le \Delta l \le 20'$	90	15	22
Strip 3	Entire strip	90	16	22
Grid 1	Entire grid	125	27	36
Strips 4A–4D	All strips	90	28	35
Strip 5A	Entire strip	−140	...	59
	Entire strip	>125	31	33
Strip 5B	Entire strip	−140	...	67
	Entire strip	>125	38	39

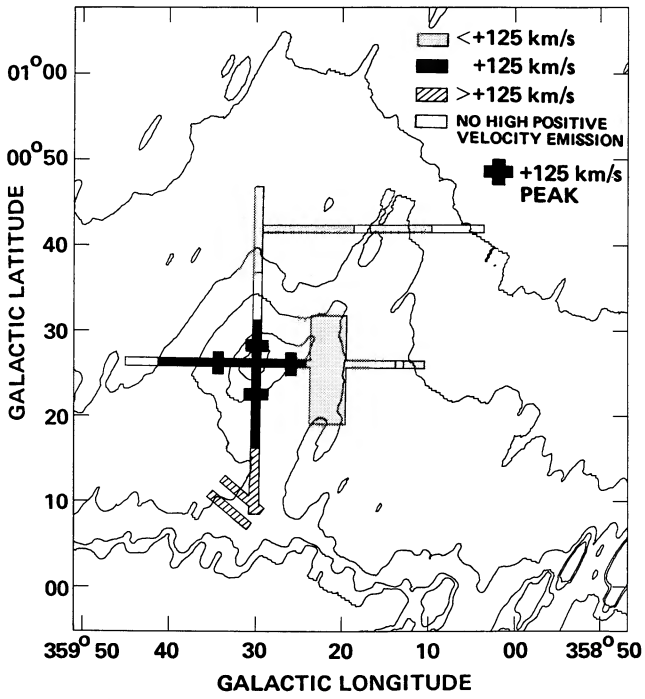

FIG. 9.—A 25 μm *IRAS* map of AFGL 5376 and the GCL showing the CO velocity trends measured in this region.

(toward increasing latitudes) and west (toward decreasing longitudes) of AFGL 5376 and is the only forbidden-velocity component in the strip crossing the GCL (strip 3). These velocities are similar to that ascribed to the Galactic center lobe by Sofue (1985).

Because the 125 km s^{-1} emission localized around AFGL 5376 is close to the velocity one would expect to see from the EMR at this projected location (Bania 1977), we suggest that AFGL 5376 is part of this large-scale feature. As part of the receding portion of the EMR, AFGL 5376 would be located beyond the Galactic center. Details of the geometry and possible relation to the western component of the GCL are discussed in § V.

IV. THE MASS OF AFGL 5376

In most circumstances, optically thick CO emission is a better indicator of the physical temperature of the gas than of its column density. In this case, it is probably neither. Although $^{12}CO(J = 2–1)$ is often optically thick near the Galactic center (and thus we assume it to be the case here), a maximum line temperature (T_A^*) of only 6 K ($T_{ex} = 13$ K) is seen around AFGL 5376, indicating that either the ambient gas is not dense enough to thermalize its states having $J \geq 2$ or is clumpy on a small scale and thus has a small beam filling factor (~ 0.25). The kinetic temperature of molecular gas in this region is typically ≥ 50 K (Morris *et al.* 1983; Güsten *et al.* 1985). Rough estimates of the mean gas density may, however, still be derived from the ^{12}CO data if we adopt a few assumptions about Galactic center molecular clouds, following the procedure of Güsten (1989).

The column density of H_2, $N(H_2)$, may be directly estimated from the integrated ^{12}CO line intensities, W_{CO}, with the following empirical relation determined by Bloemen *et al.* (1986):

$$N(H_2)/W_{CO(1-0)} = 2.8 \times 10^{20} \text{ cm}^{-2}(\text{km s}^{-1} \text{ K})^{-1} . \quad (1)$$

By comparing CO and H I survey data with γ-ray data, they find that $N(H_2)/W_{CO(1-0)}$ remains relatively constant throughout the Galaxy. For an order-of-magnitude calculation, we adopt this relation for Galactic center molecular clouds. $W_{CO(2-1)}$ was determined by integrating the line areas between 50 and 150 km s^{-1} of spectra within 6′ of the center of AFGL 5376. The above relation was applied directly to the result by assuming $W_{CO(2-1)} \simeq W_{CO(1-0)}$, a reasonable approximation if $\tau \gg 1$. The average H_2 column density is determined in this way to be $N(H_2) = 2.5 \times 10^{22}$ cm^{-2}. Using a radius of 6′ (or 15 pc at a distance of 8.5 kpc) for AFGL 5376, we derive a total cloud mass of $2.8 \times 10^5 M_\odot$ and an average H_2 density of 250 cm^{-3}. As noted earlier, ^{12}CO in dense regions like this may suffer from self-absorption. If such is the case, our mass estimate will be low, although if the relative CO abundance is higher than elsewhere in the Galaxy because of higher metallicity, then this procedure would overestimate the mass.

Two additional independent mass estimates of AFGL 5376 may be made if its gas is assumed to be either virialized or tidally stable against the strong potential gradient in the Galactic center. However, we regard such mass estimates as upper limits, because it is unlikely that these assumptions are applicable to this situation. AFGL 5376 is observed at high velocities (125 km s^{-1}) and, as evidenced in the *IRAS* images and the CO data, appears to be interacting with the surrounding gas of the GCL. AFGL 5376 may thus be a transient structure, in which case virialization or stability against tidal forces will not be a prerequisite for its existence.

First, if AFGL 5376 is stable against tidal disruption by the potential gradient near the Galactic center, then the mean H_2 density of the cloud must exceed a critical value determined by

$$\langle n \rangle_T > 10^4 \text{ cm}^{-3} * (75 \text{ pc}/R_{gc})^{1.8} , \quad (2)$$

where R_{gc} is the distance of AFGL 5376 from the Galactic center (Güsten and Downes 1980). Assuming that AFGL 5376 is located 160 pc (Bania 1977) from the Galactic center, at the estimated radius of the EMR (corrected for a Galactic center distance of 8.5 kpc), we determine that its average H_2 number density must exceed 2.6×10^3 cm^{-3} to be stable against tidal forces. This is an order of magnitude larger than the mean density derived from W_{CO}. For a spherical source with a radius of 15 pc, the minimum tidal mass of AFGL 5376 is $1.8 \times 10^6 M_\odot$.

If AFGL 5376 is instead assumed to be virialized, then the density may be estimated with the following relation:

$$\langle n \rangle_V = 10^3 \text{ cm}^{-3} * (\Delta V/R_{cl})^2 . \quad (3)$$

Here R_{cl} is the radius of the cloud and ΔV is its FWHM line width. Using the measured FWHM range of $\Delta V = 23$ to 33 km s^{-1}, we estimate an H_2 number density between $n(H_2) = 2.4 \times 10^3$ and 4.8×10^3 cm^{-3}. The virial mass of AFGL 5376 is thus between 1.7×10^6 and $3.4 \times 10^6 M_\odot$.

Following Güsten (1989) and equating the H_2 densities determined in relations (2) and (3), we can estimate the FWHM line width from a Galactic center molecular cloud using only its size and galactocentric distance:

$$\Delta V = 17 \text{ km s}^{-1} \times (R_{cl}/10 \text{ pc}) \times (150 \text{ pc}/R_{gc})^{0.9} . \quad (4)$$

With the parameters appropriate to AFGL 5376, the theoretical estimate for virialized and tidally stable gas found in this location is $\Delta V = 24$ km s^{-1}, which is within the observed FWHM from AFGL 5376, $\Delta V = 23$–33 km s^{-1}. The larger measured line widths, however, may indicate a violent origin and a possible transient nature of both the EMR and AFGL 5376 (i.e., the inapplicability of virialization and tidal stability), especially if the mean density determined from W_{CO} is approximately correct.

V. DISCUSSION: A MODEL OF AFGL 5376, THE GCL, AND SURROUNDING REGIONS

a) AFGL 5376 and the EMR

The CO data presented here demonstrate that AFGL 5376, a bright and extended infrared object, is physically located within a few hundred parsecs of the Galactic center. The CO emission which we ascribe to AFGL 5376 is centered on the infrared peak (at $l = -0.^\circ5$, $b = 0.^\circ43$) and is localized within 6′ of that peak. It has an average velocity of 125 km s^{-1} and a FWHM line width of 23–33 km s^{-1}, typical of what is seen from Galactic center molecular clouds (Bally *et al.* 1988). The color temperature of AFGL 5376 (100 K), however, exceeds that of other Galactic center molecular clouds ($T_c \simeq 40$ K), indicating an enhanced heating mechanism. A possible scenario for this heating is presented below.

The data indicate that AFGL 5376 is part of, or is associated with, the expanding molecular ring. The observed radial velocity of AFGL 5376 (125 km s^{-1}) corresponds to that of EMR material (between 115 and 165 km s^{-1}; see Fig. 12 in Bania 1977) at this projected longitude. The large positive velocity shared by these two features is opposite in sign to that expected of Galactic rotation in this region. Such a forbidden velocity is

indicative of highly noncircular motion, in this case arising from the receding portion of the EMR as it expands radially from the Galactic center. Therefore, the shared velocities of these two features imply a mutual physical association rather than coincidental alignment. The position of AFGL 5376 above the Galactic plane (at $b = 0.^{\circ}43$) is not inconsistent with the geometry of the EMR. The EMR, in addition to having its projected major axis tilted by 10° with respect to the Galactic plane, also appears to have an inclination angle of about 75° (Fig. 10*a*). This incline is evidenced by the fact that the positive velocity portion of the EMR (its receding edge) is generally confined to positive latitudes, while its negative velocity component (its forward edge) is observed at negative latitudes (Figs. 11*a* and 11*b* of Bally *et al.* 1988). Emission from the EMR is observed as far from the Galactic plane as $b = 0.^{\circ}4$, the limits of current CO survey coverage to date. AFGL 5376 may thus comprise one of the northernmost portions of the EMR.

AFGL 5376 has a minimum estimated mass of 2.8×10^5 $M_{\odot}$, a diameter of about 30 pc, and kinetic energy on the order of 10^{53} ergs, typical of what is observed in molecular clouds believed to be associated with the EMR (Bania 1977).

Although the hypothesis that the EMR is an expanding ring structure is well supported by the kinematic data (Güsten and Downes 1980), the origin of this unusual feature is not well understood. For the purpose of this discussion, we adopt the hypothesis that the EMR is the result of an energetic event that occurred within the Galactic nucleus, among which includes the possibility of a central explosion or starburst activity; this mechanism provides the most straightforward explanation for the ring symmetry and the high radial velocity of the EMR. Furthermore, the orientation of the EMR is similar to that of another large-scale gas feature, the 8.°0 radius H I disk centered on the Galactic nucleus (Liszt and Burton 1978, 1980). The shared orientation of these two features is consistent with a central explosion model in which the EMR is a postshock manifestation of an initially spherical shock front expanding through the preexisting H I disk. However, one characteristic of the EMR that complicates the question of a Galactic center origin is its longitudinal asymmetry (it extends between $-1.^{\circ}0 < l < 1.^{\circ}8$). Much of the ambient molecular gas in this region also appears to be asymmetrically distributed toward positive longitudes (Scoville, Solomon, and Jefferts 1974; Oort 1977; Bally *et al.* 1988; Heiligman 1987). Under these circumstances, an expansion feature originating from the Galactic center should then elongate toward negative latitudes, because it encounters the least amount of resistance in that direction. That the EMR is weighted toward positive longitudes is thus counter to what is expected from the given conditions. Therefore, upon adopting an explosive origin for the EMR, we are also compelled to consider the possibility that this event was offset (by as much as 60 pc eastward in projection) from the dynamical center of the Galaxy.

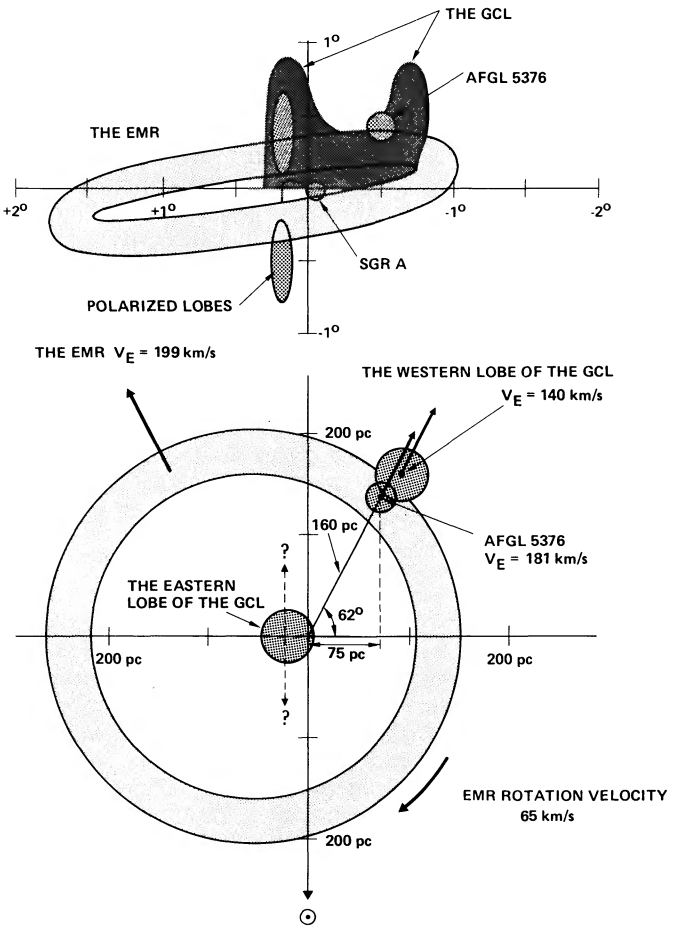

FIG. 10.—*Top*: A schematic diagram of AFGL 5376, the Galactic center lobe, and the expanding molecular ring as viewed from Earth. *Bottom*: The proposed geometry of the Galactic center features as viewed from the north Galactic pole. The galactocentric expansion velocity (V_E) is indicated for AFGL 5376, the EMR and the GCL.

b) AFGL 5376 and the Western Component of the GCL

Evidence indicates that in addition to being part of the EMR, AFGL 5376 is also physically associated with the western component of the Galactic center lobe. In the 25 μm *IRAS* map, these two features are coincident, and interaction is suggested by the alignment of the outermost noncircular contours of AFGL 5376 with the GCL. This is particularly evident in the band of emission that extends south from AFGL 5376 toward the Galactic plane (Figs. 1*c* and 2). In addition, the GCL and AFGL 5376 have in common high positive velocities that, apart from the EMR, are quite unusual to this region. The ^{12}CO data presented here indicate that the 125 km s^{-1} gas is associated with AFGL 5376, while the lower velocity 90 km s^{-1} gas is likely to be associated with the GCL. Figure 3 suggests that the envelope of emission containing these two velocity components is continuous; follow-up observations are underway to verify whether this continuity provides conclusive evidence for the association of AFGL 5376 and the GCL.

A plausible scenario which is suggested by both CO and IR data is that AFGL 5376 and the GCL are colliding with each other. The abrupt velocity jump between the 125 km s^{-1} intensity peak of AFGL 5376 and the peak of the 90 km s^{-1} gas associated with the GCL can be interpreted as a shock. However, perhaps the strongest evidence of shock activity in AFGL 5376 is its unusually high temperature of $T_c = 100$ K, which is well above the average dust temperature of $T_c \simeq 40$ K (or $T_d \simeq 27$ K, assuming a dust emission efficiency factor proportional to λ^{-2}; Cox and Laureijs 1989) observed within a few hundred parsecs of the Galactic center. The high temperature of AFGL 5376 is not easily explained otherwise; heating by massive young stars results in spatially averaged dust temperatures of $T_c = 30$–40 K (Cox, Krügel, and Mezger 1986) and is thus excluded. Besides, no indication of a compact

H II region is seen at the location of AFGL 5376 in radio continuum maps, although the ratio of far-IR and radio fluxes there is consistent with that of a normal H II region (Reich, Sofue, and Fürst 1987). There are no indications that heating by cosmic rays or X-rays could be responsible for the temperature of AFGL 5376 (via gas dust temperature coupling), unless such fluxes in the Galactic center are many orders of magnitude larger than that observed in the rest of the Galaxy (Morris *et al.* 1983). In addition, it is not clear how these or other general heating mechanisms could preferentially heat a single cloud. In order to assess the hypothesis that the heating is dominated by shocks, we are examining the presumed shock discontinuities with higher resolution CO mapping. The results will be published in a later paper.

c) AFGL 5376 as a Link Between the GCL and the EMR

If the hypotheses presented here are valid, it follows that the EMR and the GCL are also physically related by virtue of their apparent mutual association with AFGL 5376. Furthermore, both the observed velocities and the relative placement of the EMR, AFGL 5376, and the Galactic center lobe allow for a common origin of these features. Figure 10*b* illustrates the proposed geometry of AFGL 5376, the expanding molecular ring, and the Galactic center lobe. A modeled rotation velocity of 65 km s^{-1} (Bania 1977), consistent with that of earlier fits (Scoville 1972; Kaifu, Kato, and Iguchi 1972), is adopted for the EMR. AFGL 5376 and the GCL are assumed to rotate with the EMR; their average galactocentric expansion velocities in the direction of the EMR were determined accordingly. AFGL 5376 is observed west of the Galactic center at a projected distance of 75 pc. If located at the average galactocentric radius of the EMR, 160 pc (Bania 1977), AFGL 5376 lies about 140 pc beyond the Galactic center.

The data presented here suggest that gas at the forefront of the EMR, near AFGL 5376, is encountering resistance in the form of either a high-density region (clouds) or a strong magnetic field. In strip 3 (Fig. 6), the high positive velocity emission from this region appears to connect with the -70 km s^{-1} emission as well. If these apparent connections correspond to physically associated features, then we may be seeing the acceleration of the ambient gas by the EMR.

The high-velocity gas of the EMR ($V_R = 115$ to 165 km s^{-1}), upon encountering the obstruction, is deflected out of the Galactic plane, resulting in a spur that manifests itself as the western lobe of the GCL ($V_R = 90$ km s^{-1}). As the gas of the GCL is deflected out of the Galactic plane, its radial expansion rate is decreased with respect to the rest of the EMR gas, and the projected velocity of the GCL should then be correspondingly less. The positive velocity emission in strip 2 (Fig. 5) is consistent with this scenario, showing a trend of decreasing velocity toward larger latitudes. AFGL 5376, a molecular cloud of enhanced density in the EMR ($V_R = 125$ km s^{-1}), is proposed to be the singular portion of the EMR that is strongly interacting with the slower moving gas of the GCL.

d) The Nature of the GCL

A physical relation between the EMR and the GCL imposes a few constraints on the geometrical nature of the GCL. We argue that under the suggested circumstances, it is not likely that the GCL is a contiguous omega-shaped structure of limb-brightened cylindrical extrusion of gas as sometimes suggested. Rather, it is a chance juxtaposition of two unrelated, vertically projected spurs of radio-emitting gas. The separate identities of the eastern and western lobes might account for their dissimilarities discussed in § I. The high polarized eastern lobe is more likely to be a continuous extension of the nonthermal linear filaments of the Galactic center arc (Yusef-Zadeh and Morris 1988) located 30 pc in projection from the Galactic center. The western lobe, however, is associated with AFGL 5376 and the EMR, which, we have argued, lie about 160 pc from the Galactic center. Both CO line emission and IR fluxes from the western lobe dominate over those of the eastern lobe. The radio spectral index over the western lobe is flat and the emission is unpolarized. The radio continuum emission from the western lobe is, therefore, thermal in nature, as might be expected if it had originated from gas extruded from the Galactic plane by the expanding molecular ring. The large ratio of radio to far-IR flux noted by Reich, Sofue, and Fürst (1987) for the western lobe remains to be explained; we suggest that shock ionization accompanying the very high velocity shocks that are inevitable in this environment is the dominant ionization mechanism, in which case the associated far-IR luminosity is much less than would be the case if radiative ionization were responsible.

The model proposed here, in which the western lobe of the GCL is a part of the EMR, allows for a single explosive origin near the Galactic center. However, a more complicated set of events is required if one adopts the alternative view that the GCL is a complete cylindrical feature outlined by its eastern and western lobes. We argue that two explosive events will then be needed to form the GCL and the EMR. The GCL, as defined by its two lobes, is centered at $l = -0.^\circ2$, while the EMR is centered at about $l = +0.^\circ4$ (Fig. 10*a*). Given that the EMR has nearly twice the radius of the GCL and that their apparent centers of symmetry are separated in projection by $\sim 0.^\circ6$, it is difficult to imagine how both could have been created in a single event. In addition, there are constraints on the ordering and time separation between these explosive events. The spatial extent and location of the GCL is such that it is entirely contained within the EMR. It is thus unlikely that the GCL formed before the EMR, because this would pose the problem as to how a cylindrical protrusion of gas could have survived the passage of the EMR, or at least why it is not distorted by such a passage. On the other hand, the GCL could not have formed long after the EMR, unless the EMR is a long-lasting resonant feature (Bania 1977). The direct expansion times of the EMR (10^6 yr) and the GCL (0.44 to 2×10^6 yr: Umemura *et al.* 1988; Sofue 1985) are comparable.

The most prevalent theories on the origin of the GCL have employed energetic activity near the Galactic center or the twisting of magnetic fields by Galactic rotation to describe the GCL as a complete, large-scale feature. Such origins, however, also result in a structure that is symmetrically positioned with respect to the Galactic center. The GCL obviously does not fulfill this condition; it exists almost entirely at positive Galactic latitudes. The only exception is its eastern lobe, where the polarized emission continues as the linear filaments of the radio arc down to negative latitudes. *IRAS* maps show a similar north-south asymmetry of the GCL. It is not evident why the GCL should exhibit such asymmetry, given the apparent symmetry of the molecular gas distribution about the Galactic plane (see Table 1 of Bally *et al.* 1988). This inconsistency weakens the argument that the two lobes of the GCL constitute a complete large-scale structure.

The existence of two similar radio spurs which are physically separated but which are projected to look like a single, coher-

ent structure may not be an unreasonable demand. In *IRAS* and radio continuum maps (Fig. 1 of Downes *et al.* 1978), one finds that prominent spurs arising from the Galactic plane are not uncommon. These infrared and radio spurs may be a consequence of both the energetic, noncircular gas flows in the galactic center and the presence of strong poloidal magnetic fields to guide this material out of the plane. Further examination of the far-IR spurs is being done to better determine their nature, and the results will be presented in future paper (Uchida and Morris 1989).

VI. CONCLUSION

The Galactic center lobe (GCL) and the expanding molecular ring (EMR) are remarkable examples of the unusual, energetic activity that is occurring near the Galactic center. Based on a study of ^{12}CO in AFGL 5376, an extended *IRAS* source located near the intersection of the GCL and the EMR, we reach the following conclusions.

1. AFGL 5376, an unusually warm (100 K) and massive molecular cloud ($2.8 \times 10^5\ M_\odot$), is located near the Galactic center.

2. AFGL 5376, the large-scale expanding molecular ring, and the westernmost portion of the Galactic center lobe are associated and may have arisen from a single explosive event at the Galactic nucleus.

3. The interrelationships of these features indicate that the GCL is not likely to be a complete large-scale structure as often suggested. The double-lobed appearance of the GCL may be instead the result of a superposition of two unrelated vertically projected spurs from the Galactic plane.

We would like to thank Kenneth Young for his assistance at the CSO. This research was supported in part by NSF grants AST 87-18068 and AST 88-15132.

REFERENCES

Bally, J., Stark, A. A., Wilson, R. W., and Henkel, C. 1987, *Ap. J. Suppl.*, **65**, 13.
———. 1988, *Ap. J.*, **324**, 223.
Bally, J., and Yusef-Zadeh, F. 1989, *Ap. J.*, **336**, 173.
Bania, T. M. 1977, *Ap. J.*, **216**, 381.
Bloeman, J. G. B. M., *et al.* 1986, *Astr. Ap.*, **154**, 25.
Cohen, R. J., and Davies, R. D. 1979, *M.N.R.A.S.*, **186**, 453.
Cox, P., and Laureijs, R. 1989, in *IAU Symposium 136, The Center of the Galaxy*. ed. M. Morris (Dordrecht: Kluwer), p. 121.
Cox, P., Krügel, E., and Mezger, P. G. 1986, *Astr. Ap.*, **155**, 380.
Downes, D., Goss, W. M., Schwarz, U. J., and Wouterloot, J. G. A. 1978, *Astr. Ap. Suppl.*, **35**, 1.
Ellison, B. N., and Miller, R. E. 1987, *Internat. J. Infrared Millimeter Waves*, **8**, 609.
Güsten, R. 1989, in *IAU Symposium 136, The Center of the Galaxy*, ed. M. Morris (Dordrecht: Kluwer), p. 89.
Güsten, R., and Downes, D. 1980, *Astr. Ap.*, **87**, 6.
Güsten, R., Walmsley, C. M., Ungerechts, H., and Churchwell, E. 1985, *Astr. Ap.*, **142**, 381.
Heiligman, G. M. 1987, *Ap. J.*, **314**, 747.
Heyvaerts, J., Norman, C., and Pudritz, R. E. 1988, *Ap. J.*, **330**, 718.
Hiromoto, N., Maihara, T., Mizutani, K., Takami, H., Shibai, H., and Okuda, H. 1984, *Astr. Ap.*, **139**, 309.
Kaifu, N., Kato, T., and Iguchi, T. 1972, *Nature Phys. Sci.*, **238**, 105.
Little, S. J., and Price, S. 1985, *A.J.*, **90**, 1812.
Liszt, H. S., and Burton, W. B. 1978, *Ap. J.*, **226**, 790.
———. 1980, *Ap. J.*, **236**, 779.
Morris, M., Polish, N., Zuckerman, B., and Kaifu, N. 1983, *A.J.*, **88**, 1228.
Oort, J. H. 1977, *Ann. Rev. Astr. Ap.*, **15**, 295.
Reich, W., Sofue, Y., and Fürst, E. 1987, *Pub. Astr. Soc. Japan*, **39**, 573.
Robinson, B. J., and McGee, R. X. 1970, *Australian J. Phys.*, **23**, 405.
Sanders, R. H. 1989, in *IAU Symposium 136, The Center of the Galaxy*, ed. M. Morris (Dordrecht: Kluwer), p. 77.
Sanders, R. H., and Wrixon, G. T. 1974, *Astr. Ap.*, **33**, 9.
Scoville, N. Z. 1972, *Ap. J. (Letters)*, **175**, L127.
Scoville, N. Z., Solomon, P. M., and Jefferts, K. B. 1974, *Ap. J. (Letters)*, **187**, L63.
Scoville, N. Z., Solomon, P. M., and Thaddeus, P. 1972, *Ap. J.*, **172**, 335.
Seiradakis, J. H., Lasenby, A. N., Yusef-Zadeh, F., Weilebinski, R., and Klein, U. 1975, *Nature*, **317**, 697.
Shibata, K. 1989, in *IAU Symposium 136, The Center of the Galaxy*, ed. M. Morris (Dordrecht: Kluwer), p. 313.
Sofue, Y. 1984, *Pub. Astr. Soc. Japan*, **36**, 539.
———. 1985, *Pub. Astr. Soc. Japan*, **37**, 697.
Sofue, Y., and Handa, T. 1984, *Nature*, **310**, 568.
Tsuboi, M., Inoue, M., Handa, T., and Kato, T. 1985, *Pub. Astr. Soc. Japan*, **37**, 359.
Tsuboi, M., Inoue, M., Handa, T., Tabara, H., Kato, T., Sofue, Y., and Kaifu, N. 1986, *A.J.*, **92**, 818.
Uchida, K., and Morris, M. 1988, abstract presented at IAU Symposium No 136, The Galactic Center.
———. 1989, in preparation.
Uchida, Y., Shibata, K., and Sofue, Y. 1985, *Nature*, **317**, 699.
Umemura, S., Iki, K., Shibata, K., and Sofue, Y. 1988, *Pub. Astr. Soc. Japan*, **40**, 25.
Yusef-Zadeh, F., and Morris, M. 1988, *Ap. J.*, **329**, 729.

MARK MORRIS and KEVEN UCHIDA: Department of Astronomy, University of California at Los Angeles, Math Sciences Building, Los Angeles, CA 90024

E. SERABYN: Division of Physics, Mathematics, and Astronomy, California Institute of Technology, Downs Laboratory of Physics, 320-47, Pasadena, CA 91125